COMPUTATIONAL SIMULATION OF TURBULENT MIXING WITH MASS TRANSFER

Project F004

Report 3

to the

MEMBER COMPANIES OF THE INSTITUTE OF PAPER SCIENCE AND TECHNOLOGY

March 1998

INSTITUTE OF PAPER SCIENCE AND TECHNOLOGY

Atlanta, Georgia

COMPUTATIONAL SIMULATION OF TURBULENT MIXING WITH MASS TRANSFER

Project F004

Report 3

A Progress Report

to the

MEMBER COMPANIES OF THE INSTITUTE OF PAPER SCIENCE AND TECHNOLOGY

By

Wang, X., Feng, Z., and Forney, L.J.

March 1998

Computational Simulation of Turbulent Mixing with Mass Transfer

Xiaodong Wang †, Zhigang Feng ‡, and Larry J. Forney *

Institute of Paper Science and Technology &

Georgia Institute of Technology

Atlanta, GA 30318

Abstract

In this paper, we present a series of computational simulations of three-dimensional turbulent mixing with mass transfer for various pipe mixing arrangements. The simulations are carried out with the ADINA software, in which general-purpose finite element and finite volume formulations along with the k-ϵ turbulent model are used for incompressible Navier-Stokes flows with mass transfer. Based on the predicted pressure and velocity profiles and the standard deviation of tracer (or fiber) spatial distributions at certain distances downstream from the injection point, we compare the mixing performances of various transverse, concentric, and multijet mixers as well as four silo mixing units. In addition, we deduce certain design information pertaining to different mixing configurations.

---

† Assistant Professor, IPST

‡ Research Associate, IPST

* Associate Professor, School of Chemical Engineering

1 Introduction

Turbulent mixing of various fluid streams has many industrial applications in areas such as sewer discharge, chemical reactions, heat transfer operations, and mixing and combustion processes [5] [12]. In the paper industry, fiber water mixture needs to be diluted and delivered smoothly and uniformly to the headbox forming section. One of the key components is the so-called silo mixing unit depicted in Fig. 1, which consists of various pipe mixing arrangements. In this work, we consider the following mathematical models related, but not limited to current silo designs: (i) transverse mixers at different injection angles; (ii) concentric mixers with different nozzle shapes; and (iii) multijet mixers. Full-fledged simulations for four silo mixing units with complex three-dimensional geometries are also investigated. Considering the fact that the rheology of low consistency fiber water mixture is very similar to that of water, we employ the mixing model of two turbulent miscible fluids with the same density and viscosity, however, different inert tracer concentrations.

In the general area of turbulent mixing, many research efforts have been directed to experimental investigations. Recently, some numerical studies have been performed on two- or three-dimensional turbulent mixing with mass or heat transfer for simple geometries [10]. However, very few studies are available for dealing with complex three-dimensional turbulent simulation with mass transfer. Some of the recent advances in applying CFD techniques to the chemical process industry are documented in Ref. [11]. In this paper, we present a systematic study of various fundamental pipe mixers and silo mixing units using the ADINA software, which consists of the program on heat transfer in solids ADINA-T, the program on displacements and stresses ADINA, the program on fluid flows and heat transfer ADINA-F, the pre-processor ADINA-IN, and the post-processor ADINA-PLOT. All the solid

model geometries used in this paper are created with the ProENGINEER software, and their corresponding meshes are generated with the automatic mesh generation algorithm in ADINA-IN. A detailed description of the recent development of the ADINA-F program is available in Ref. [1].

In the following section, we summarize the governing equations and the criteria used in measuring mixing uniformity. We discuss in Section 3 transverse jet mixers with different angles. In Section 4, we focus on concentric mixers with various nozzle shapes. The relatively new multijet mixing arrangements are considered in Section 5, and the full-fledged silo mixing unit simulations are presented in Section 6. Design information deduced from the computational simulation results is presented in Sections 3 to 6 as well as in the concluding section.

2 Research Approaches

We consider here the turbulent flow of a homogeneous, viscous, incompressible fluid with constant properties. By representing the fluctuating parts in the eddy viscosity ν_t, turbulent kinetic energy k, and turbulent dissipation rate ϵ, we obtain the following governing equations from the mass and momentum conservation equations [7] [14]:

$$\begin{aligned} \frac{\partial v_i}{\partial x_i} &= 0 \\ \frac{\partial v_i}{\partial t} + v_j \frac{\partial v_i}{\partial x_j} &= \frac{1}{\rho}\frac{\partial p}{\partial x_i} + \frac{\partial}{\partial x_j}((\nu + \nu_t)\frac{\partial v_i}{\partial x_j}) \end{aligned} \tag{1}$$

where ρ, ν, ν_t, v_i, and p stand for fluid mass density, kinematic viscosity, eddy viscosity, time-average fluid flow velocity in direction x_i, and time-average pressure, respectively. Furthermore, for the standard k-ϵ turbulent model, we have two additional equations:

$$\begin{aligned} \frac{\partial k}{\partial t} + v_j \frac{\partial k}{\partial x_j} &= \frac{\partial}{\partial x_j}((\nu + \frac{\nu_t}{\sigma_k})\frac{\partial k}{\partial x_j}) + \nu_t \Phi - \frac{k}{T} \\ \frac{\partial \epsilon}{\partial t} + v_j \frac{\partial \epsilon}{\partial x_j} &= \frac{\partial}{\partial x_j}((\nu + \frac{\nu_t}{\sigma_\epsilon})\frac{\partial \epsilon}{\partial x_j}) + a_1 \frac{1}{T}\nu_t \Phi - a_2 \frac{\epsilon}{T} \end{aligned} \tag{2}$$

where a_1, a_2, σ_k, and σ_ϵ are designated constants; Φ denotes the inner product of the velocity strain tensor $2e_{ij}e_{ij}$ with $e_{ij} = (\frac{\partial v_i}{\partial x_j} + \frac{\partial v_j}{\partial x_i})/2$; and the turbulent time scale T and viscosity ν_t are expressed as:

$$T = \frac{k}{\epsilon} + \sqrt{\frac{\nu}{\epsilon}} \tag{3}$$

$$\nu_t = c_\mu k T \tag{4}$$

with a constant c_μ.

In addition to the mass and momentum conservation equations with the k-ϵ turbulent model, we employ the following tracer conservation equation to model the mass transfer phenomena in the turbulent flow,

$$\frac{\partial c}{\partial t} + v_j \frac{\partial c}{\partial x_j} = \frac{\partial}{\partial x_j}((\nu/Sc + \nu_t/\sigma_c)\frac{\partial c}{\partial x_j}) \tag{5}$$

where c, Sc, and σ_c are the time-average concentration of tracer (or fiber), Schmidt number, and a selected constant. We note that a similar equation can be directly obtained for the temperature distribution in the case of heat transfer.

The governing equations (1), (2), and (5) are implemented in the ADINA-F program. Moreover, the turbulent diffusivity $\nu/Sc + \nu_t/\sigma_c$ as a function of spatial locations is incorporated in the user-supplied subroutine provided by the ADINA software. In this work, we select $a_1 = 1.44$, $a_2 = 1.92$, $\sigma_k = 1.0$, $\sigma_\epsilon = 1.3$, $c_\mu = 0.09$, $Sc = 1.64 \times 10^6$, and $\sigma_c = 0.9$. The modification of these constants based on the experimental validation will be reported in a forthcoming paper.

The mixing uniformity is measured in terms of two relative standard deviations σ_c and σ_{cu} of the concentration c with respect to the arithmetic mean $\bar{c}$. We define $\bar{c}$, σ_c, and σ_{cu} at a certain pipe cross section A downstream from the nozzle as follows:

$$\bar{c} = \int_A c dA \Big/ \int_A dA \tag{6}$$

$$\sigma_c^2 = \int_A (\frac{c-\bar{c}}{\bar{c}})^2 dA \Big/ \int_A dA \tag{7}$$

$$\sigma_{cu}^2 = \int_A (\frac{c-\bar{c}}{\bar{c}})^2 u dA \Big/ \int_A u dA \tag{8}$$

We recognize that the integrals $\int_A u dA$ and $\int_A cu dA$ are directly related to the volume flow rates and tracer concentration through mass balances. Denoting q and Q as the flow rates of the streams with tracer concentrations c_1 and c_2, respectively, from the mass conservation laws, we obtain

$$\int_A u dA = q + Q \tag{9}$$

$$\int_A cu dA = c_1 q + c_2 Q \tag{10}$$

which can be used to validate the computational results.

3 Transverse Mixers

The most widely used pipe mixer is the transverse mixer shown in Fig. 2, in which a jet with diameter d_1 issues fluid containing tracer into a tube of diameter d_2. The ambient fluid velocity of the tube is v_2, and the initial tracer jet velocity is v_1.

We compare, in this work, transverse mixers with the following physical parameters: $d_1 = 0.1092$ m; $d_2 = 0.3048$ m; $v_1 = 3.0$ m/s; $v_2 = 1.0$ m/s; $c_1 = 0.03$; $c_2 = 0$; and consequently $q = \frac{\pi}{4} d_1^2 v_1 = 0.2810 \times 10^{-1}$ m^3/s; $Q = \frac{\pi}{4} d_2^2 v_2 =$

0.7297×10^{-1} m^3/s. Figure 3 shows the solid models of transverse mixers with various jet injection angles. In order to compare the mixing efficiency of various transverse mixers, we present in Fig. 4 the quantitative measures based on the computational results at the corresponding cut planes. In the subplots $\int_A udA$ and $\int_A cudA$, the numerical results are compared with the references derived from the mass conservation laws in Eqs. (9) and (10). In addition, the subplot $\int_A cdA/A$ represents the uniformity of the mixing, and the subplot $\int_A cudA/A$ stands for the average tracer mass flow rate. Figures 5 and 6 depict the mass-ratio contours and pressure distributions for transverse mixers with different injection angles. It is clearly shown in Fig. 5 and the subplots σ_c^2 and σ_{cu}^2 in Fig. 4 that the mixing efficiency of the pipe mixer with a 90^o injection angle is better than that of the mixers with acute angles, and by pointing the injection jet upstream, i.e., $\theta > 90^o$, only slight improvement can be achieved. This conclusion correlates with the experimental finding discussed in Ref. [9]. However, in the paper industry, in addition to the mixing efficiency, we also have to consider the large-scale vortices where fiber flocks or bundles may form. As is clearly indicated in Fig. 6, significant circulations or vortices can exist near the injection point due to the adverse pressure gradient in transverse pipe mixers with right or obtuse injection angles. Furthermore, to avoid having the jet impact on the wall and consequently create the pressure pulsation and flow disturbance in the approach flow system, we may have to consider the jet trajectory. It is shown from the absolute velocity band plots in Fig. 7 that the jet trajectories of the transverse mixers with acute injection angles are less likely to impact the opposite wall. More detailed information on the jet trajectory is available in Refs. [3] and [6].

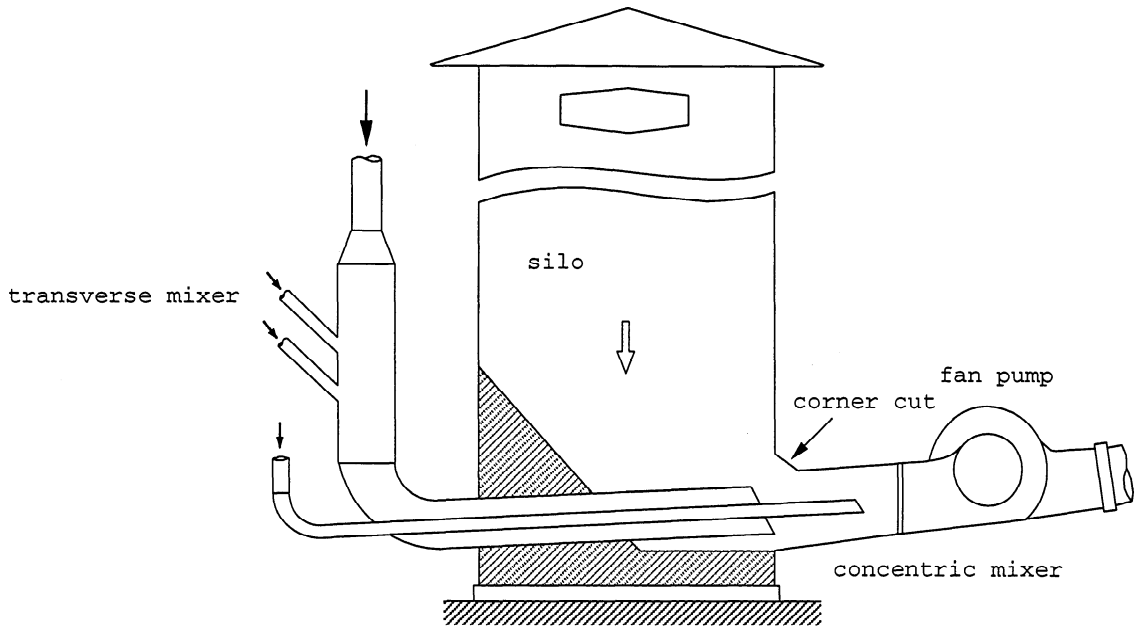

Figure 1: A typical silo pipe mixing system.

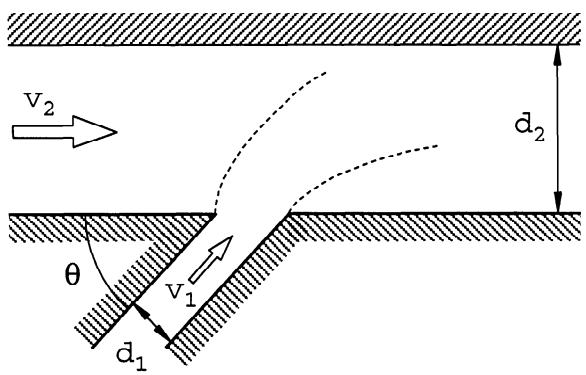

Figure 2: A typical transverse pipe mixing model.

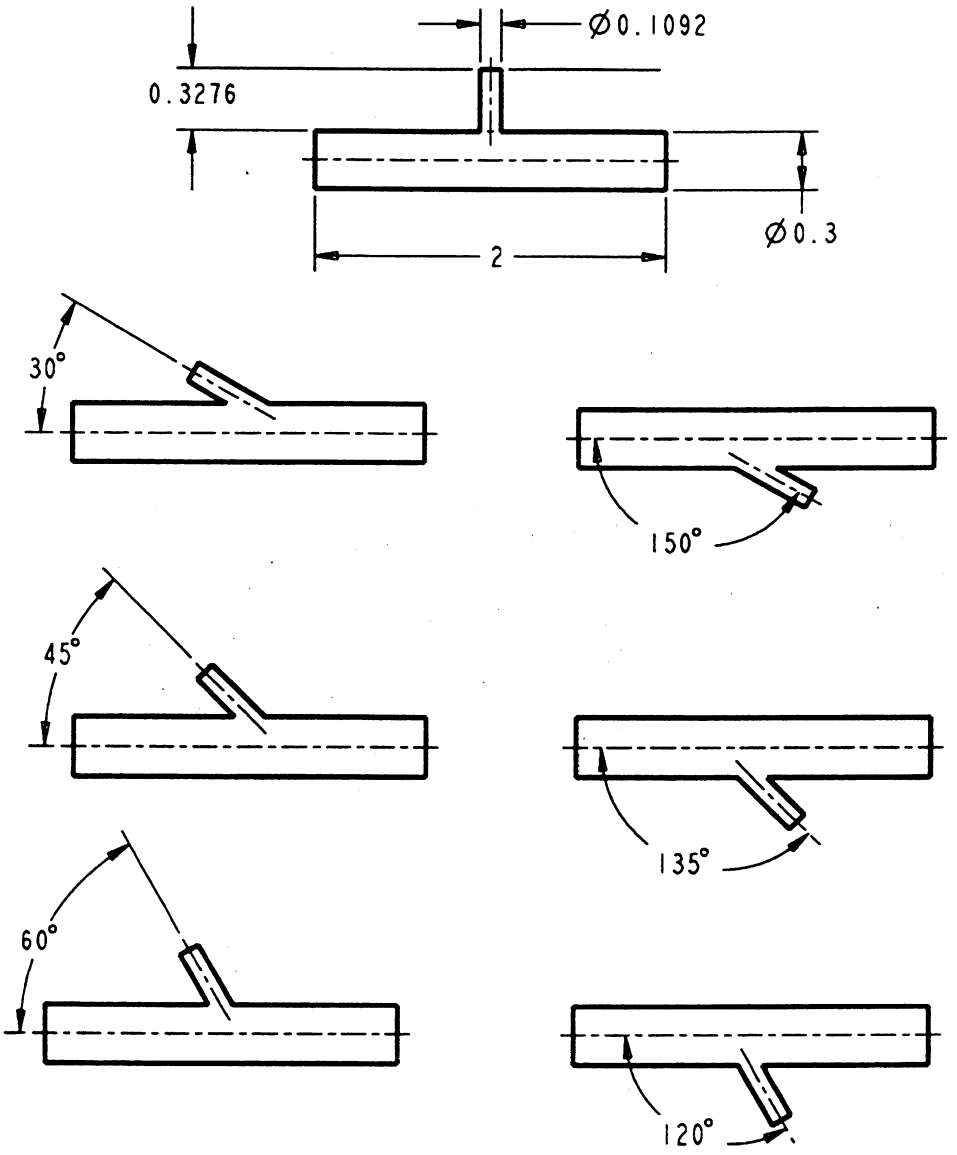

Figure 3: Solid models of transverse mixers with various jet injetion angles.

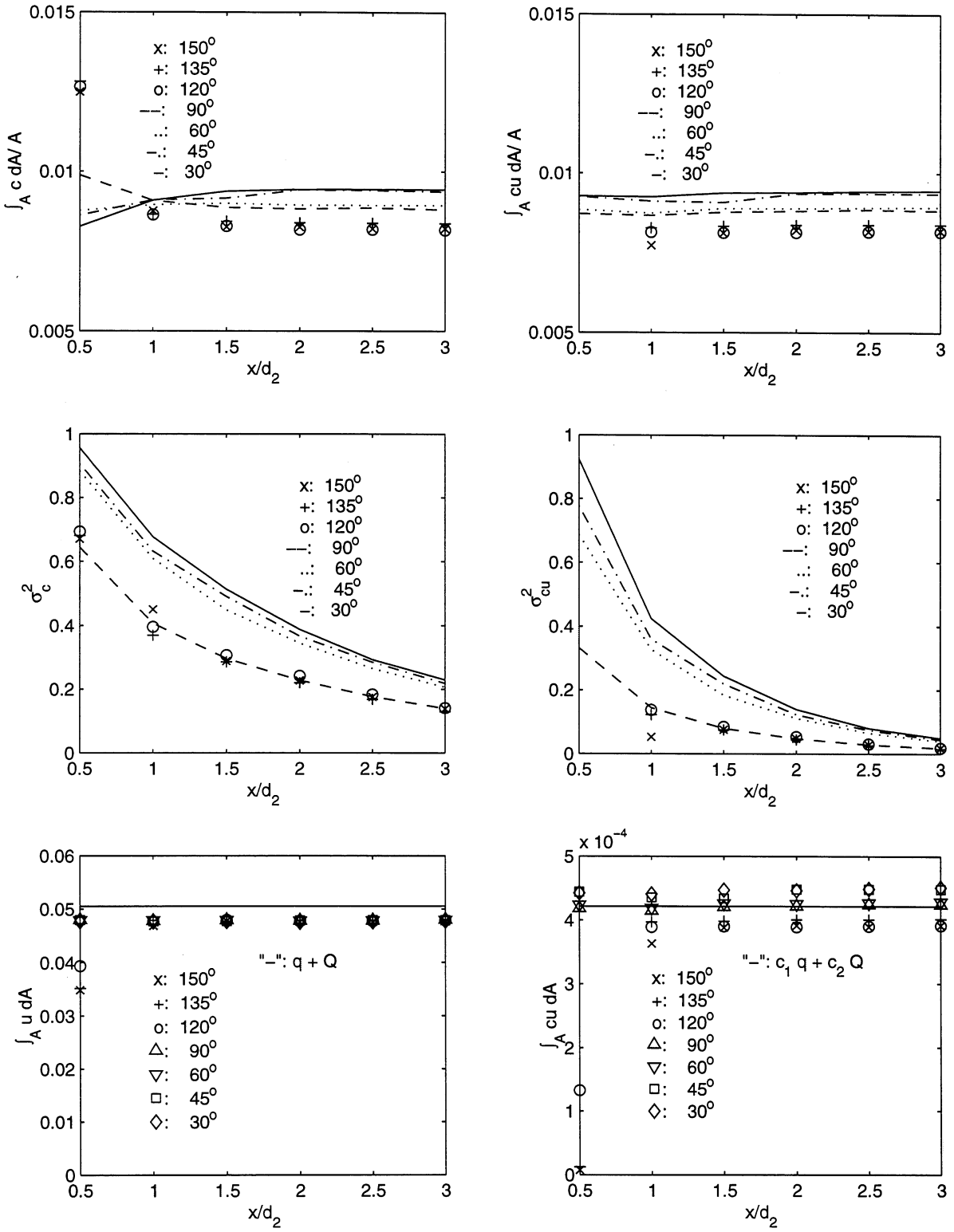

Figure 4: Mixing uniformity measures of various transverse pipe mixers.

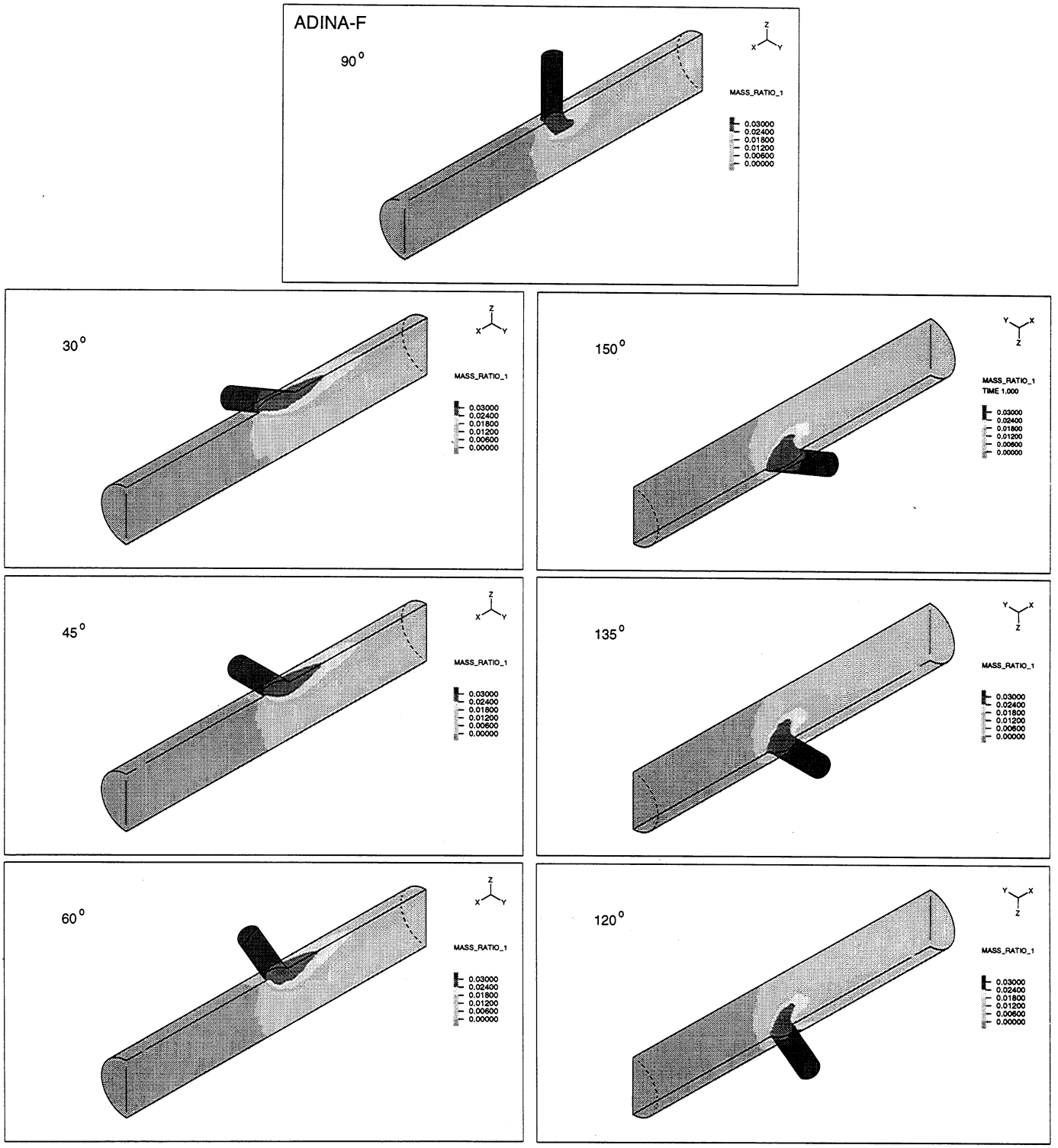

Figure 5: Tracer distribution (mass-ratio) of transverse pipe mixers with various injection angles.

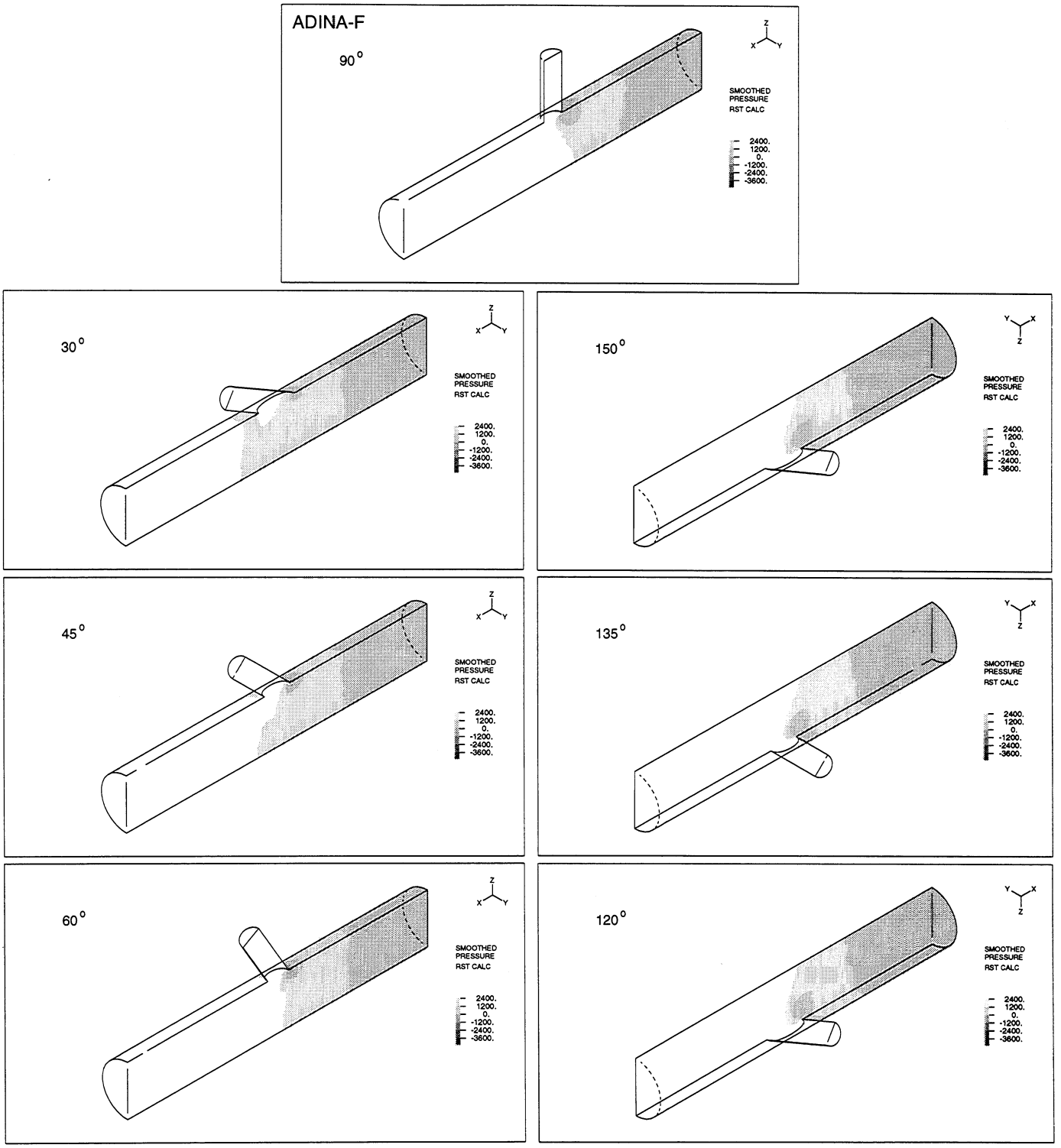

Figure 6: Pressure band plots of transverse pipe mixers with various injection angles.

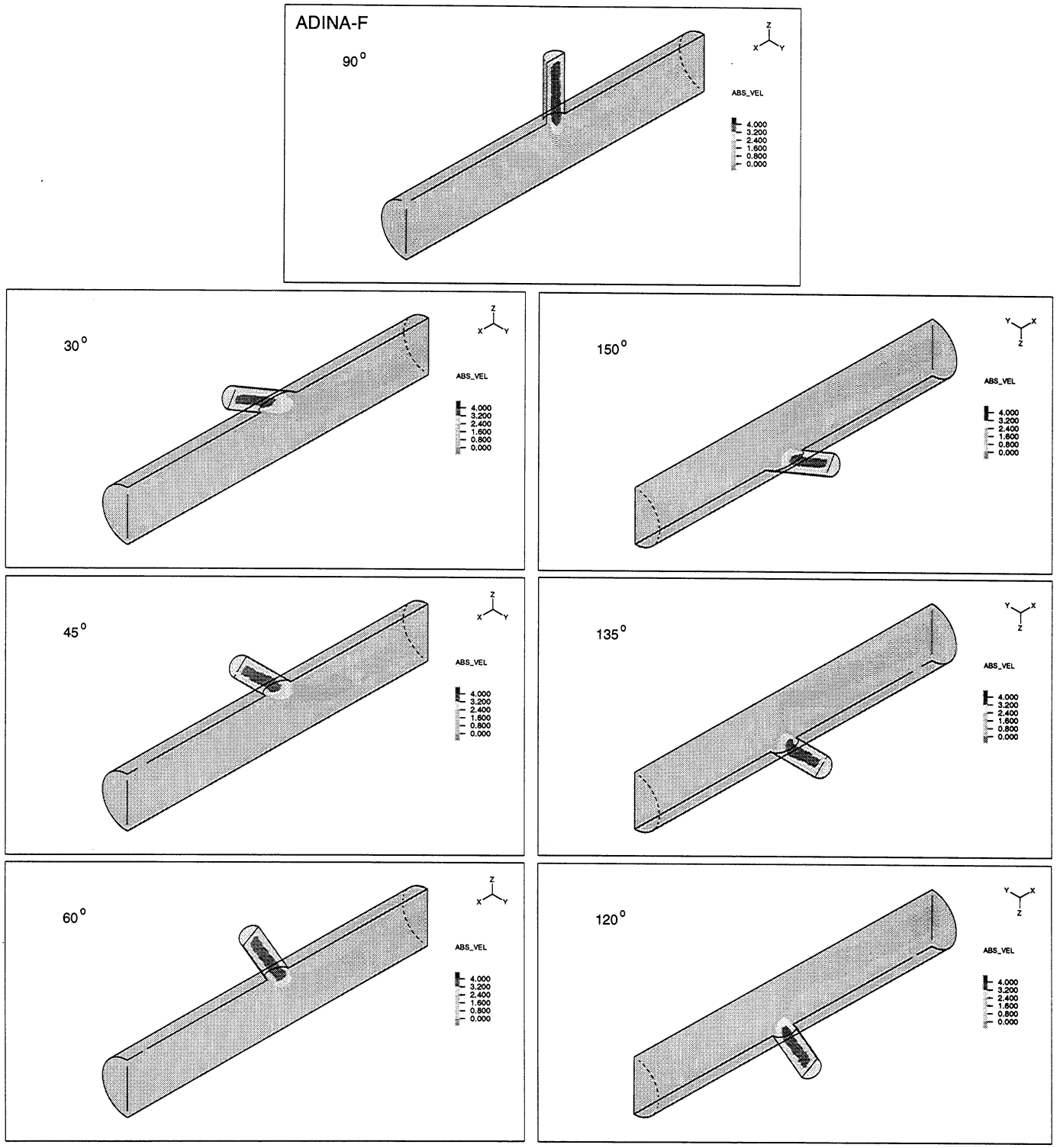

Figure 7: Velocity contour of transverse pipe mixers with various injection angles.

4 Concentric Mixers

In the paper industry, concentric mixers are also used extensively. An early computational study on this subject is presented in Ref. [4]. In the concentric mixers depicted in Fig. 8, two pipes are installed coaxially with the smaller one contained in the large one, and fiber stock within the small pipe is injected into the large pipe, which normally contains low consistency fiber stock or white water with a lower velocity. The possible design variations of concentric mixers are the nozzle cut angle θ and nozzle shape.

We compare concentric mixers with the following physical parameters: $d_{1i} = 0.1092$ m; $d_{1o} = 0.1244$ m; $d_2 = 0.3048$ m; $v_1 = 3.0$ m/s; $v_2 = 1.2$ m/s; $c_1 = 0.03$; $c_2 = 0$; and consequently, $q = \frac{\pi}{4} d_{1i}^2 v_1 = 0.2810 \times 10^{-1}$ m^3/s; $Q = \frac{\pi}{4}(d_2^2 - d_{1o}^2)v_2 = 0.7297 \times 10^{-1}$ m^3/s. Figure 9 shows the solid models of four concentric mixers with various jet nozzles. The quantitative measures at the corresponding cut planes are presented in Fig. 10. Figure 11 depicts the mass-ratio contours of four concentric mixers. It is interesting to note that in this set of configurations commonly used by the paper industry, the concentric pipe mixer is more effective than the transverse pipe mixer, and the nozzle shapes do not affect the mixing very much. This conclusion is counterintuitive concerning the existing knowledge in various chemical engineering areas where the tangential mixing efficiency is only one sixth of the normal mixing efficiency [6]. Nevertheless, we notice that the ratio of the injection jet radius and the main pipe radius in such chemical engineering problems is often small, i.e., the jet is in effect issued into an infinite body of fluid, which is not the case in the paper industry. Of course, further work must be done to optimize these geometries, that is, for a fixed flow ratio q/Q and distance-to-mixing ratio x/d_2, the optimum diameter ratio must be determined to minimize the

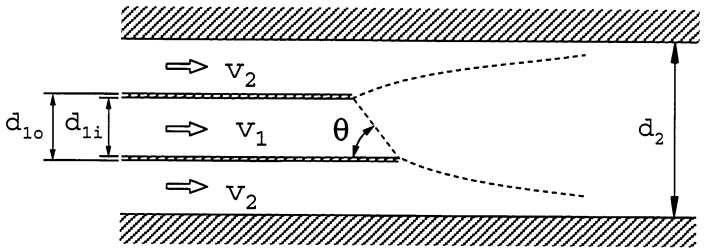

Figure 8: A typical concentric pipe mixing model.

variation coefficients σ_c and σ_{cu}.

To further the investigation of nozzle shape effects, we compute another set of geometry and velocity ratios. As can be seen from Figs. 12 and 13, the mixing efficiency of the contracting nozzle is much better than that of flat nozzles with various cut angles.

5 Multijet Mixers

As a relatively new mixing idea, multiple jets are often used to impinge on each other to create a more efficient mixing zone. Early experimental and computational studies are reported in Refs. [2] and [8]. It is conceivable that in the near future multijet mixers will be introduced in the paper industry along with the current coaxial and transverse mixers.

In this work, we compare three multijet mixers (2, 3, and 4 jets) with the corresponding transverse mixer with a 90^o injection angle. Different multijet mixers are indicated with the jet number n. The physical parameters are listed as follows: $d_1 = 0.7722 \times 10^{-1}$ m; $d_2 = 0.3048$ m; $v_2 = 1.0$ m/s; $c_1 = 0.03$; $c_2 = 0$; and consequently $q = n\frac{\pi}{4}d_1^2 v_1 = 0.2810 \times 10^{-1}$ m^3/s; $Q = \frac{\pi}{4}d_2^2 v_2 = 0.7297 \times 10^{-1}$ m^3/s. We vary the jet velocity v_1 corresponding to the jet number n in order to preserve the constant flow rate q. Figure 15 shows the solid models of three multijet mixers.

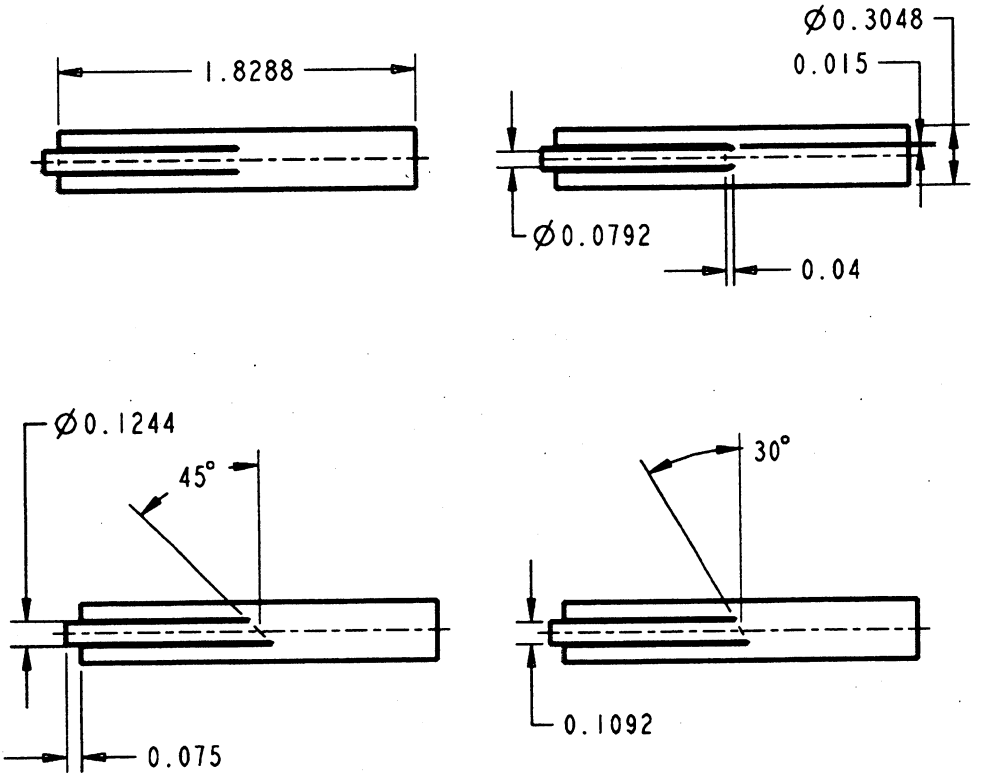

Figure 9: Solid models of concentric pipe mixers with various nozzle designs.

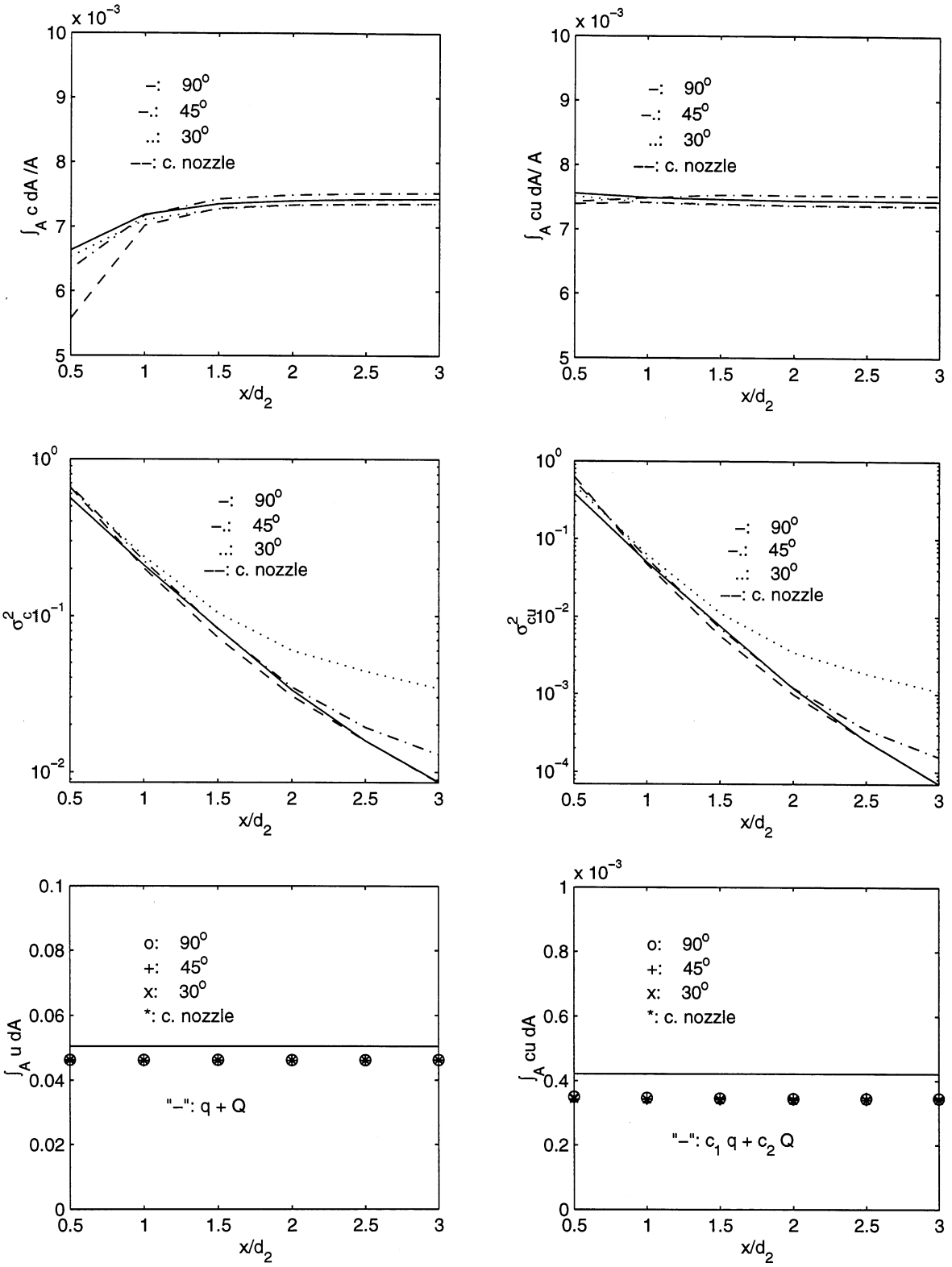

Figure 10: Measures of mixing uniformity of various concentric pipe mixers.

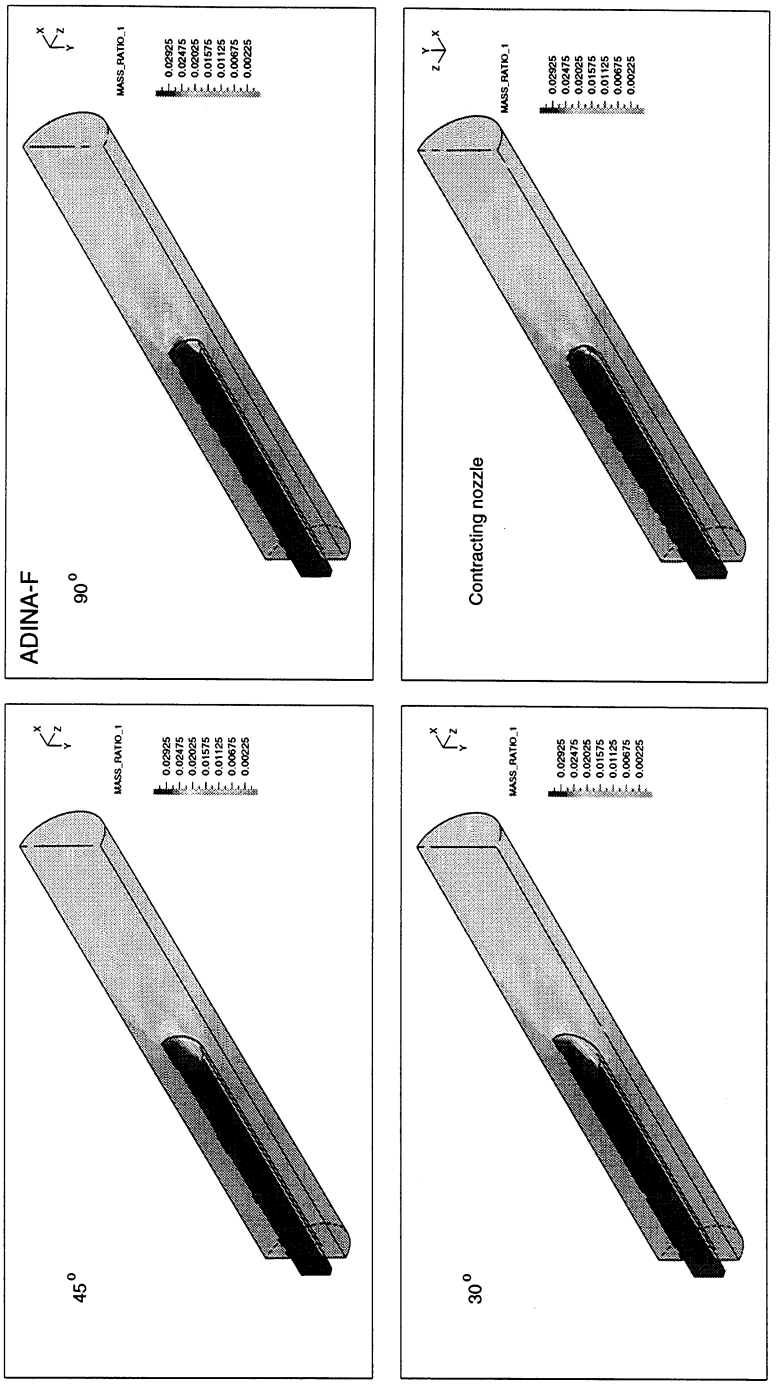

Figure 11: Tracer distribution (mass-ratio) of various concentric pipe mixers.

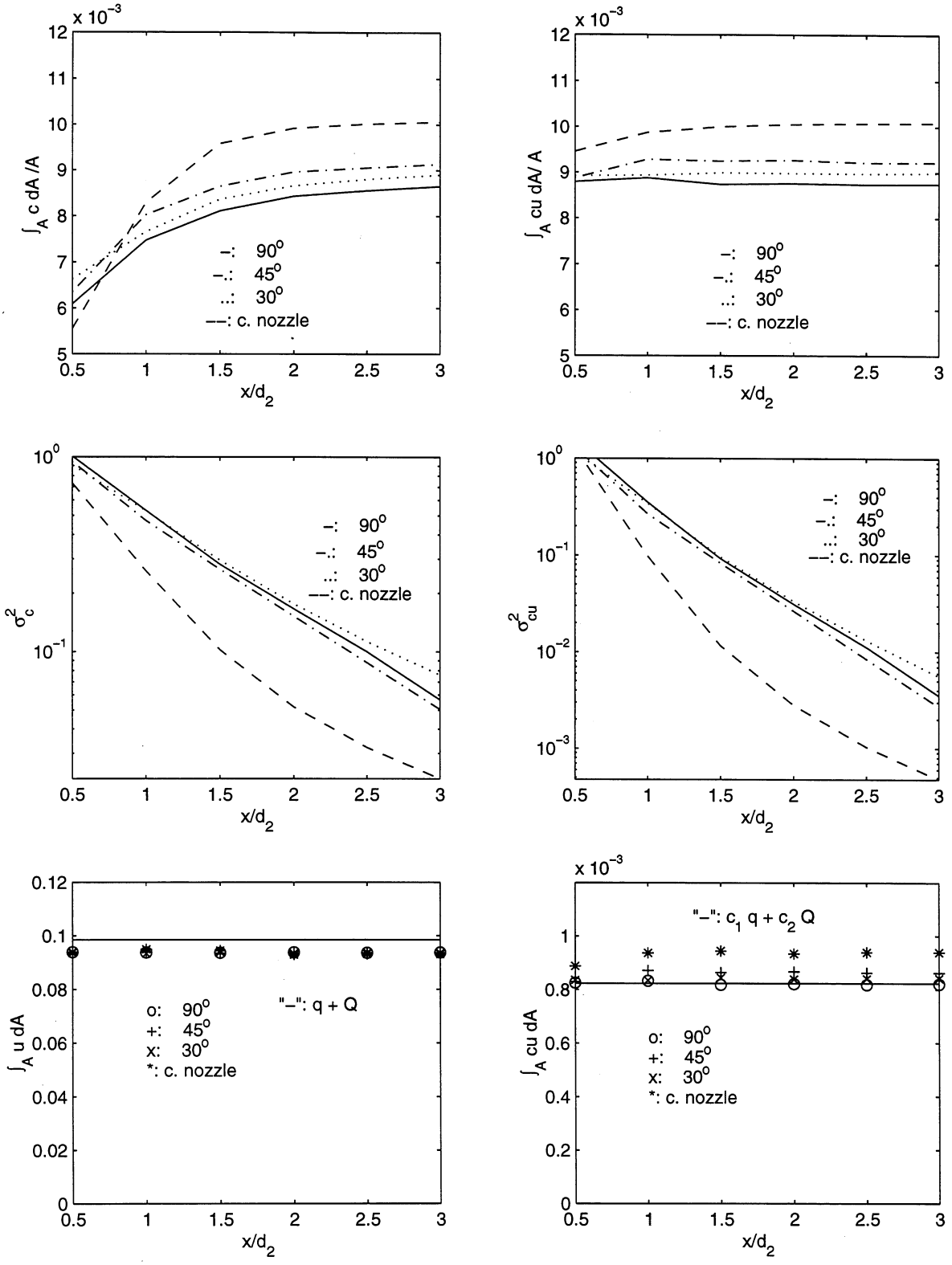

Figure 12: Measures of mixing uniformity of various concentric pipe mixers. ($d_{1i} = 0.1526$ m; $d_{1o} = 0.1676$ m; $d_2 = 0.4572$ m; $v_1 = 3.0$ m/s; $v_2 = 1.0$ m/s.)

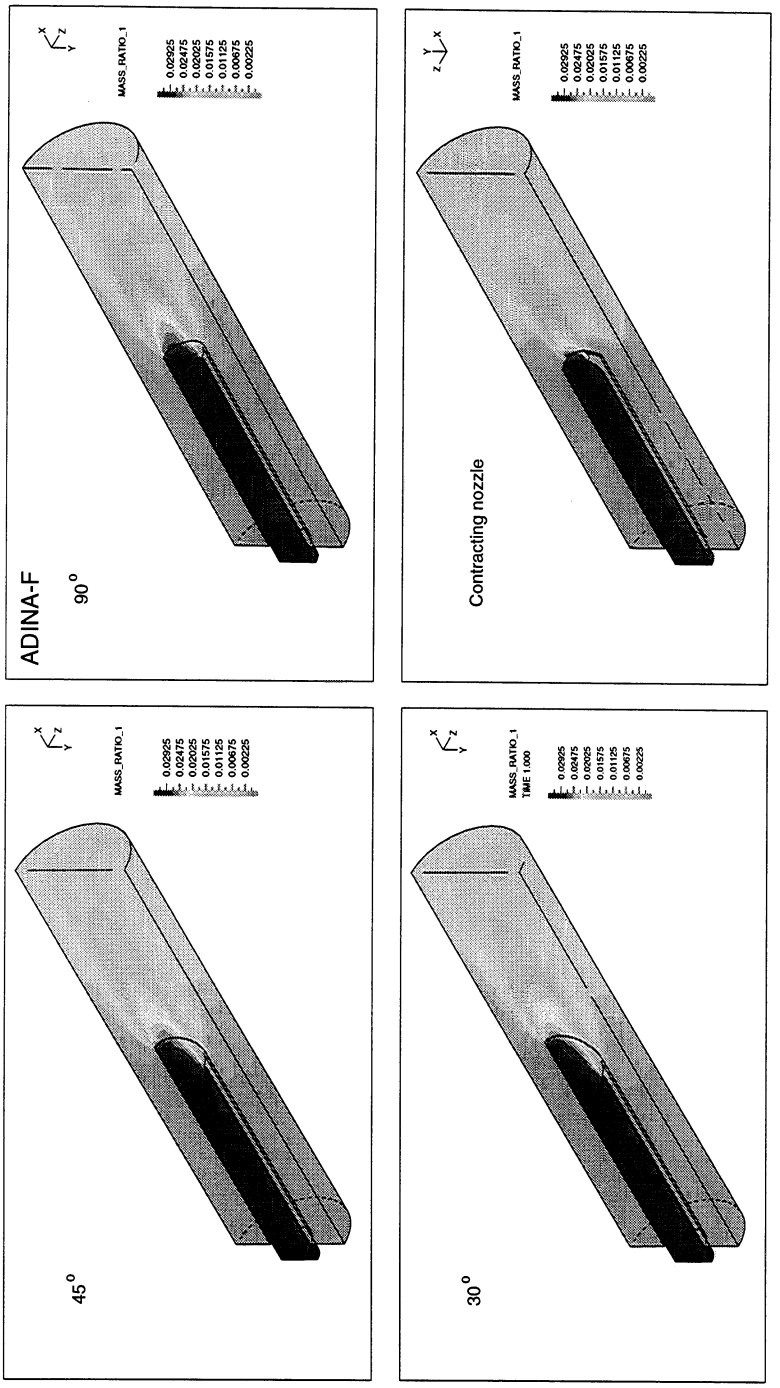

Figure 13: Tracer distribution (mass-ratio) of various concentric pipe mixers with different ratio of inner and outer pipe radii. ($d_{1i} = 0.1526$ m; $d_{1o} = 0.1676$ m; $d_2 = 0.4572$ m; $v_1 = 3.0$ m/s; $v_2 = 1.0$ m/s.)

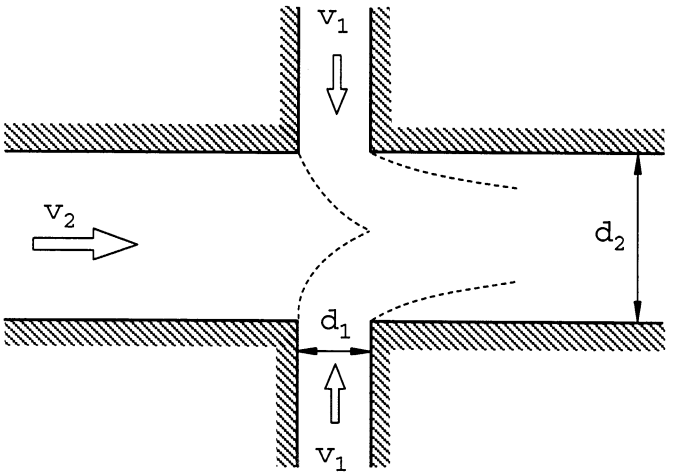

Figure 14: A typical multijet pipe mixing model.

The quantitative measures at the corresponding cut planes are shown in Fig. 16. Figure 17 depicts the mass-ratio distributions of multijet mixers along with the corresponding transverse mixer with a 90^o injection angle. Compared with the single transverse jet mixer, the mixing efficiency of multijets is much better. It is also interesting to note that multijets with an even number of jets perform better than those with an odd number of jets. For example, although more jets within the multijet mixer imply better mixing, a two-jet mixer achieves better mixing than a three-jet mixer for $x/d_2 > 1.5$.

6 Silo Unit

As illustrated in the mathematical model depicted in Fig. 18, the silo is a cylindrical water storage tank with a constant water level. The inner pipe protruding into the fan pump inlet zone contains a higher consistency fiber stock (e.g., 3%), and the concentric outer pipe collects the recirculation diluted stock (e.g., 2%). In this paper, we assume that the concentric pipes are rigid. The issue of dynamic instability of

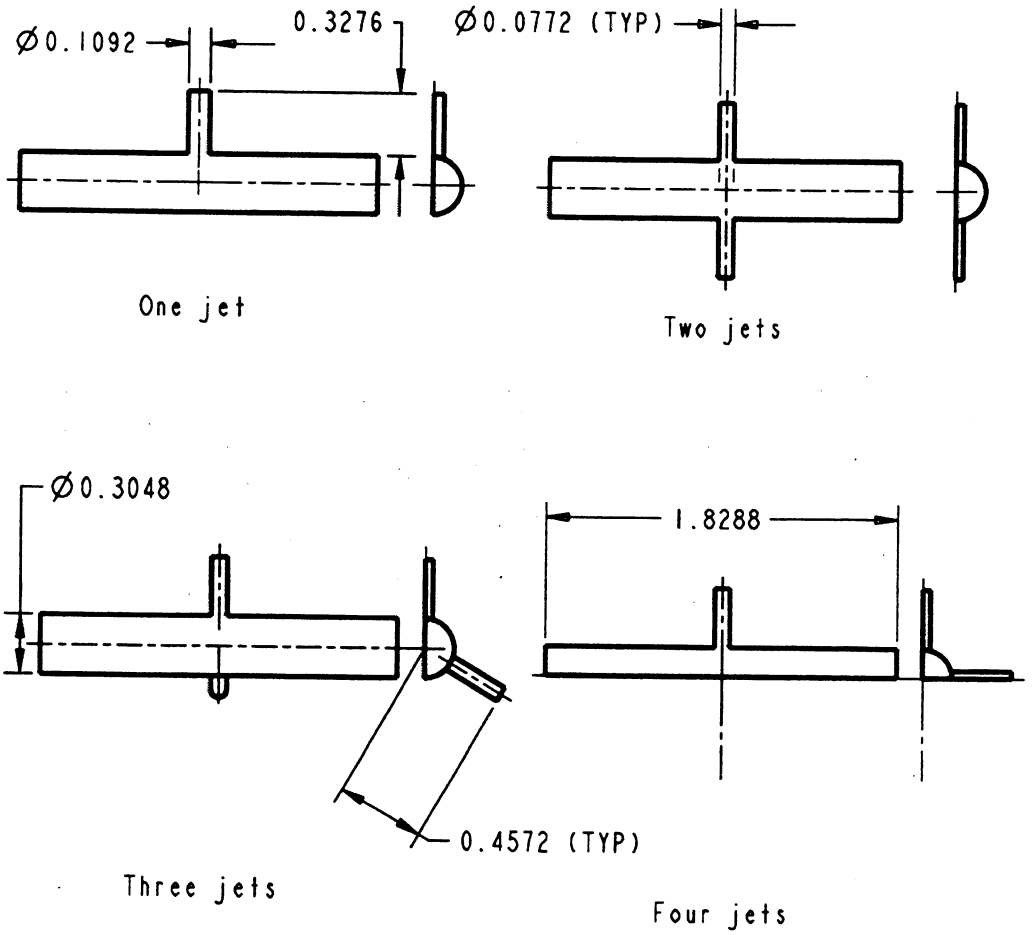

Figure 15: Solid models of various designs of multijet pipe mixers.

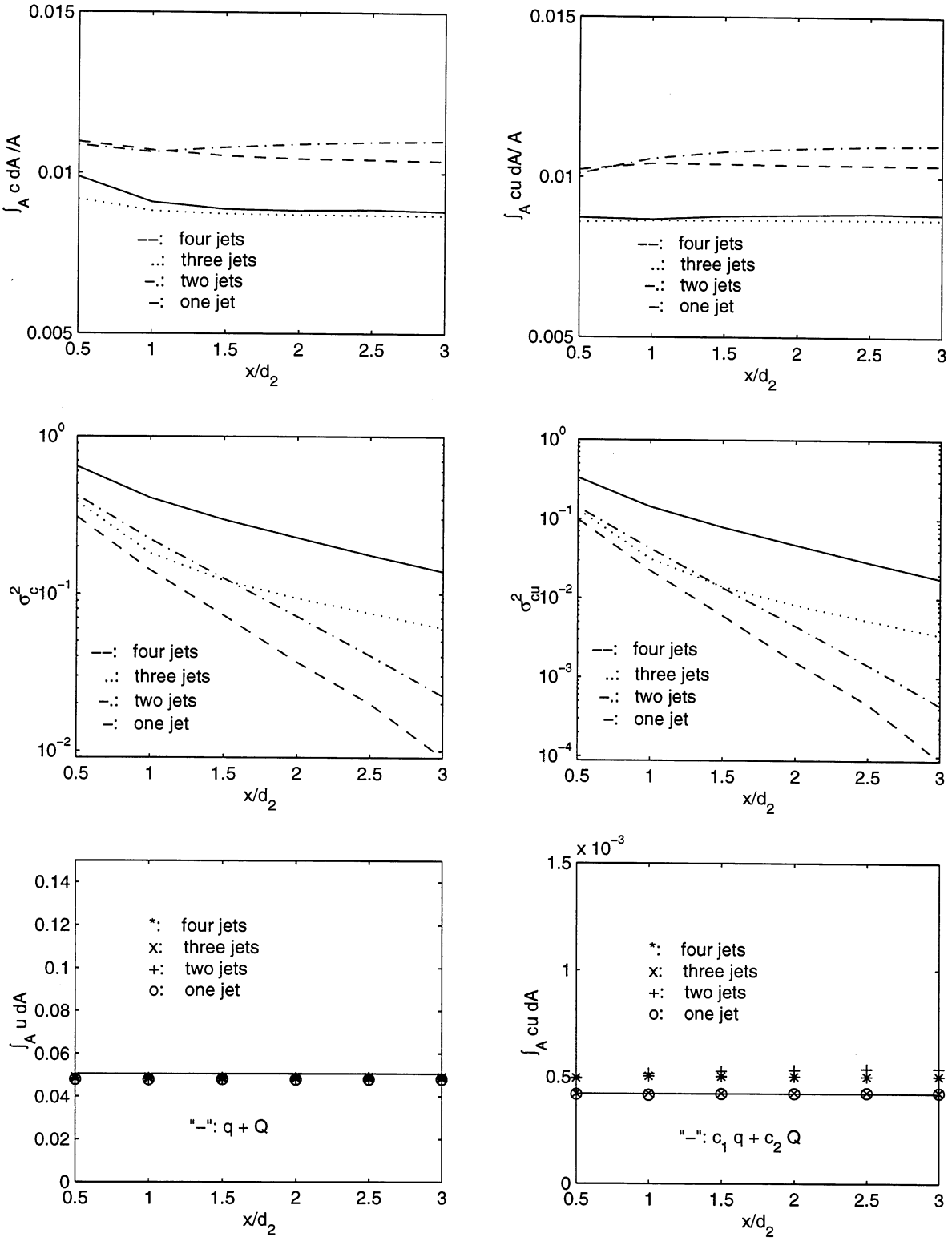

Figure 16: Measures of mixing uniformity of various multijet pipe mixers.

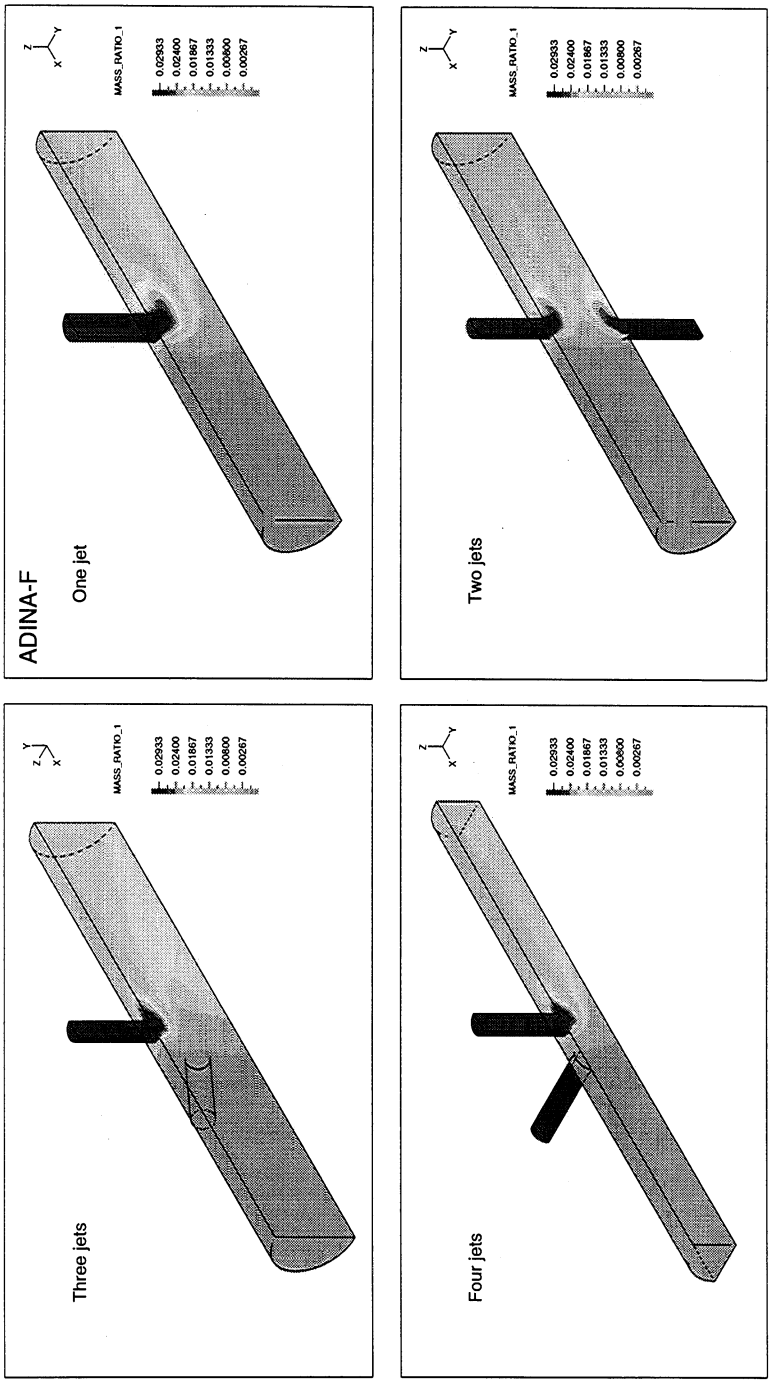

Figure 17: Tracer distribution (mass-ratio) of various multijet pipe mixers.

these suspended pipes is addressed in Ref. [13].

Industry research suggests that the fan pump location can directly affect the paper sheet formation. Although many practical aspects, including the suspended pipe vibration, may contribute to smooth pump operation or even sheet property variations, in this work, we focus on the issues of fan pump location, i.e., the length of the outlet pipe, and the corner cut (a common practice in the paper industry). Therefore, the basic consideration is the same as those for transverse, concentric, or multijet mixers, where the mixing uniformity is measured at a certain distance downstream from the injection point.

We consider four silo units illustrated in Fig. 19. The inner and outer pipe flow velocities are 1 and 3 m/s, respectively, and the equivalent velocity for the silo water supply from the top is 0.0349 m/s. Case A represents the initial design configuration. Case B includes the modification with a corner cut. Case C has a longer outlet pipe. Case D combines two modifications in Cases B and C together. Figure 19 shows the solid models of four silo units. The quantitative measures at the corresponding cut planes for each case are presented in Fig. 20. Figure 21 presents the mass-ratio contours at six different axial locations (cut surfaces) of the outlet pipe in four silo units. It is evident, by comparing Cases B, C, and D with Case A, that mixing efficiency can be significantly improved by the elongation of the outlet pipe; also, the corner cut is not a dominant factor. In fact, in the subplots σ_c^2 and σ_{cu}^2 in Fig. 20, if we compare Case A with Case B or Case C with Case D, we find that the corner cut enhances rather than reduces the concentration nonuniformity.

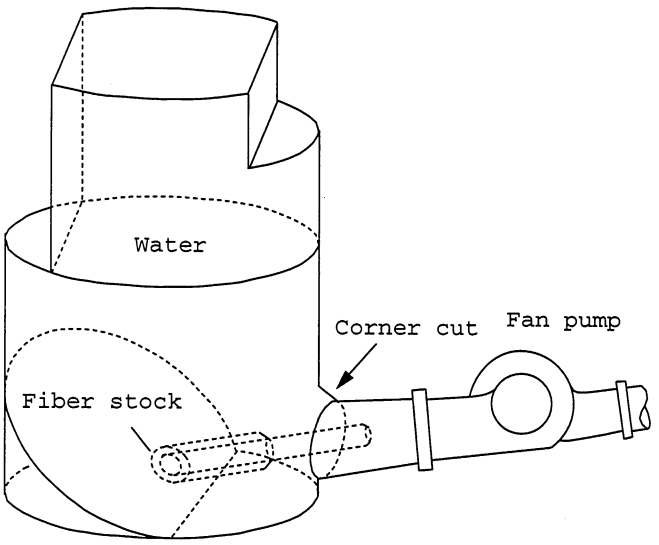

Figure 18: A typical silo pipe mixing unit model.

7 Conclusions

In this paper, a systematic numerical study of various pipe mixers and silo mixing units has been conducted with the ADINA software. To summarize, we obtain the following information pertaining to the design of the considered mixing arrangements:

(1) Although transverse mixers with an injectction angle of $\theta \geq 90^o$ are more efficient in mixing, they tend to produce large-scale vortices near the injection point, and the jet is more susceptible to impacting the opposite wall. Therefore, in the paper industry, an acute injection angle may be considered, and in practice, a longer distance downstream away from the injection point is recommended in order to compensate for the loss of mixing efficiency.

(2) In concentric mixers, with the same input flow rates, for the geometries used in this work (typical geometries in the paper industry), the mixing efficiency is much higher than those of the corresponding transverse and multijet mixers. In addition, from the further investigation with different relative injection jet size, we find that

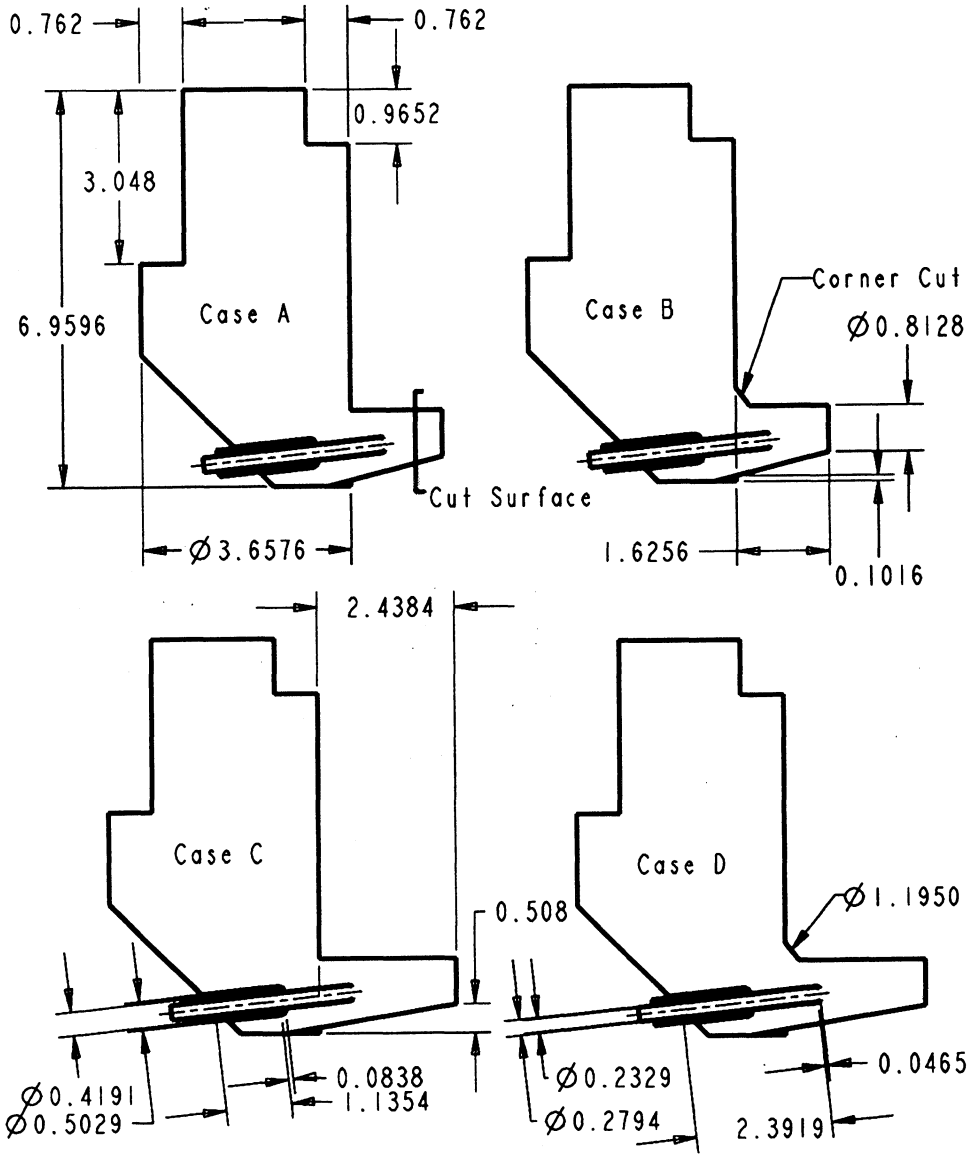

Figure 19: Solid models of various modifications of silo pipe mixing models.

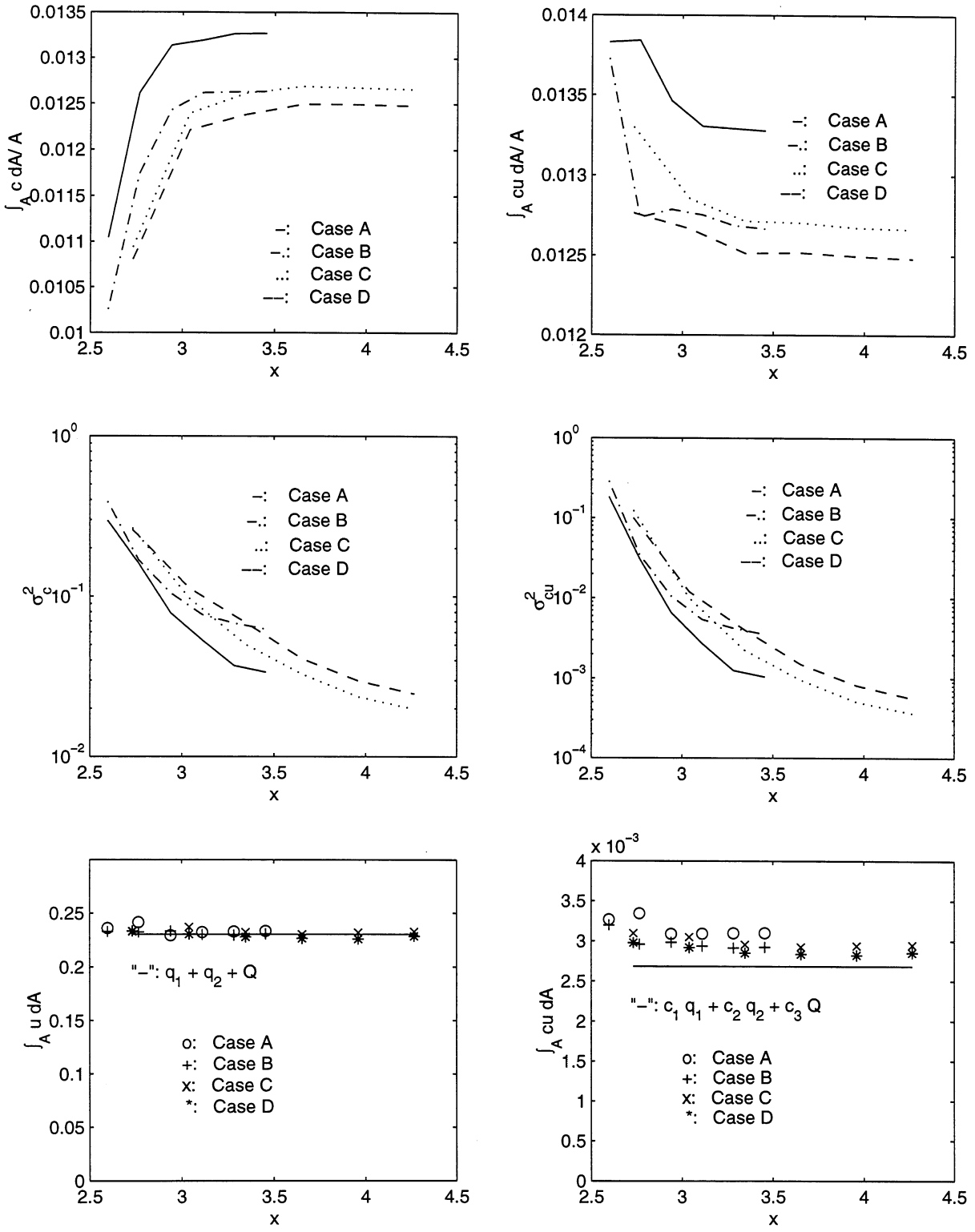

Figure 20: Measures of mixing uniformity of various silo pipe mixing arrangements. (q_1 and q_2 are the flow rates of the inner and outer concentric pipes, and Q is the flow rate of the silo. c_i is the corresponding fiber consistency.)

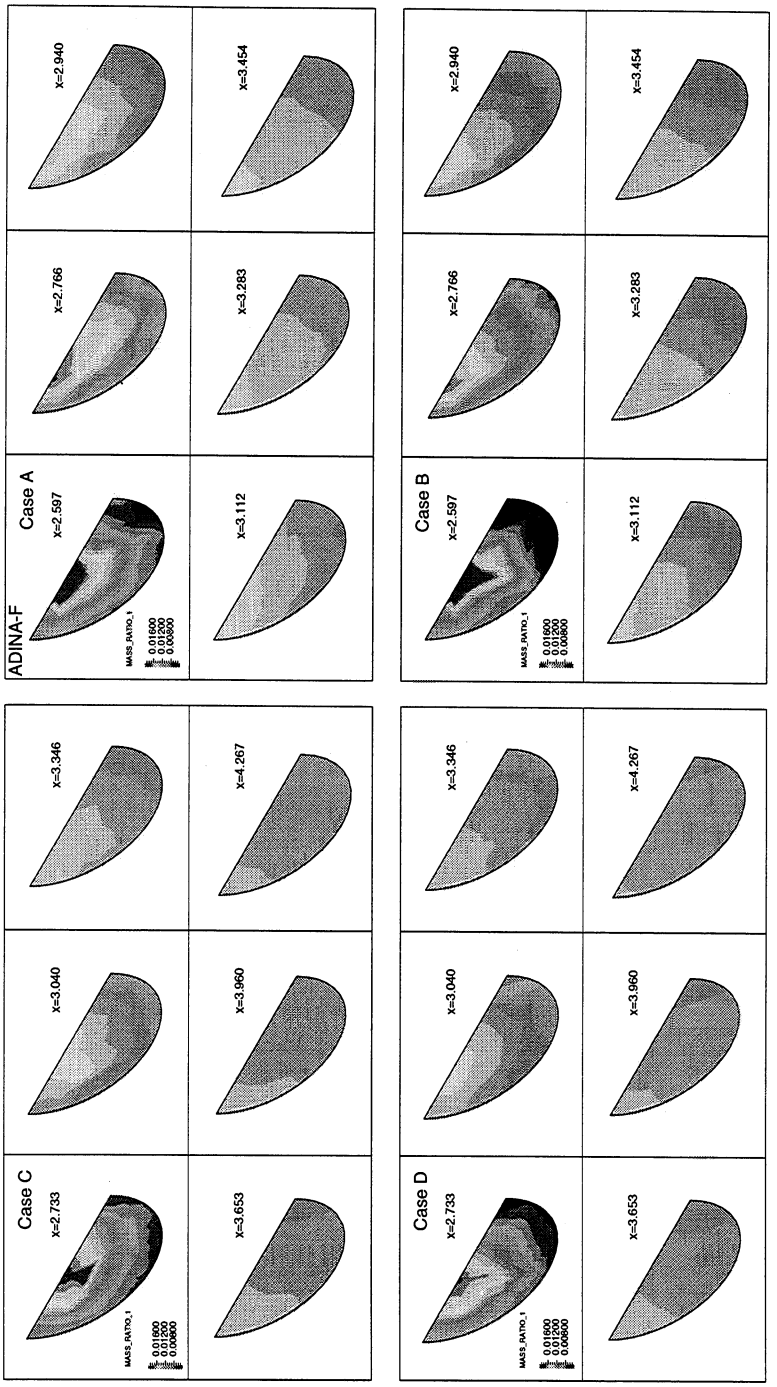

Figure 21: Tracer distribution (mass-ratio) at various cut planes of four silo units. Each case has six cut surfaces represented by their x-coordinates and the last one coincides with the end of the silo outlet pipe.

mixing efficiency can be greatly improved in the case of the contracting nozzle. This indicates that in the case of mixing chemical additives, the contracting nozzle is recommended. In general, a flat nozzle with various cut angles θ does not affect mixing significantly.

(3) Multijet mixing is, in general, better than single jet mixing, and an even number of jets is recommended.

(4) In the silo mixing unit design, increasing the outlet pipe length has a much greater and more positive effect on the mixing efficiency than the corner cut.

8 Acknowledgment

We would like to thank the Institute of Paper Science and Technology and the School of Chemical Engineering at the Georgia Institute of Technology for their support. We also would like to thank Mr. Andy Brown at the Institute of Paper Science and Technology for creating the ProENGINEER solid models, and the researchers in ADINA R&D, Watertown, MA, for helpful suggestions.

References

[1] K.J. Bathe, H. Zhang, and X. Zhang. Some advances in the analysis of fluid flows. *Computers & Structures*, 64(5/6):909–930, 1997.

[2] Y.R. Chang and K.S. Chen. Prediction of opposing turbulent line jets discharged laterally into a confined crossflow. *International Journal of Heat Mass Transfer*, 38(9):1693–1703, 1995.

[3] Z. Feng, X. Wang, and L.J. Forney. Single jet mixing at arbitrary angle in turbulent tube flow. *ASME Fluids Engineering Division*, 1998. FEDSM98-4890.

[4] P. Givi and J.I. Ramos. On the calculation of heat, mass and momentum transport in coaxial jets and mixing layers. *Int. Comm. Heat Mass Transfer*, 12:323–336, 1985.

[5] J.B. Gray. Turbulent radial mixing in pipes. In V.W. Uhl and J.B. Gray, editors, *Mixing: Theory and Practice Vol. III*, pages 63–130. Academic Press, 1986.

[6] D.P. Hoult, J.A. Fay, and L.J. Forney. A theory of plume rise compared with field observations. *Journal of the Air Pollution Control Association*, 19(8):585–590, 1969.

[7] B.E. Launder and D.B. Spalding. The numerical computation of turbulent flows. *Computer Methods in Applied Mechanics and Engineering*, 3:269–289, 1974.

[8] T. Maruyama, T. Mizushina, and S. Hayashiguchi. Optimum conditions for jet mixing in turbulent pipe flow. *International Chemical Engineering*, 23(4):707–716, 1983.

[9] T. Maruyama, T. Mizushina, and F. Watanabe. Turbulent mixing of two fluid streams at an oblique branch. *International Chemical Engineering*, 22(2):287–294, 1982.

[10] L.A. Monclova and L.J. Forney. Numerical simulation of a pipeline tee mixer. *Industrial Engineering Chemistry Research*, 34:1488–1493, 1995.

[11] A. Shanley. Pushing the limits of CFD. *Chemical Engineering*, pages 66–67, December 1996.

[12] L.M. Sroka and L.J. Forney. Fluid mixing with a pipeline tee: Theory and experiment. *AIChE Journal*, 35(3):406–414, 1989.

[13] X. Wang and F. Bloom. Flow induced oscillations of submerged and inclined concentric pipes with different lengths. *Journal of Fluids and Structures*, 1998. Submitted.

[14] D.C. Wilcox. *Turbulence Modeling for CFD.* DCW Industries, Inc., second edition, 1994.